AD-A092 791 DELAWARE UNIV NEWARK DEPT OF CIVIL ENGINEERING F/G 8/3
LABORATORY DRIFT-VELOCITY DISTRIBUTION AT WAVE BREAKING POINT W--ETC(U)
MAY 80 T SUNAMURA, D YANG, H WANG N00014-76-C-0342
UNCLASSIFIED OCEAN ENGINEERING-22 NL

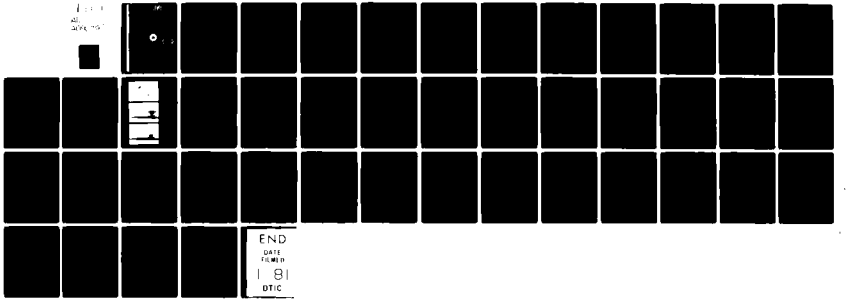

END
DATE FILMED
1 81
DTIC

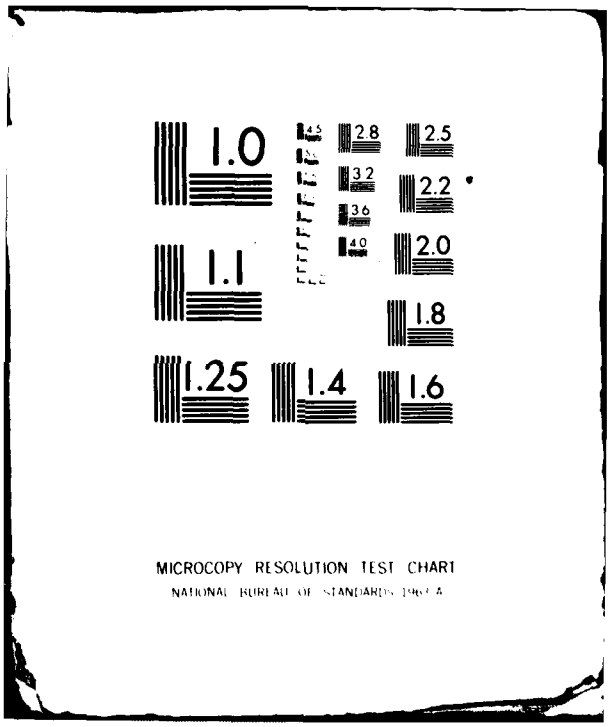
1.0
1.1
1.25
1.4
1.6
1.8
2.0
2.2
2.5
2.8
3.2
3.6
4.0
MICROCOPY RESOLUTION TEST CHART
NATIONAL BUREAU OF STANDARDS 1963 A

LEVEL II

LABORATORY DRIFT-VELOCITY DISTRIBUTION AT WAVE BREAKING POINT WITH SOME IMPLICATIONS TO SEDIMENT TRANSPORT PROCESSES

by

Tsuguo Sunamura, David Yang and Hsiang Wang

Technical Report No. 5
Contract No. N00014-76-C-0342
with the OFFICE OF NAVAL RESEARCH GEOGRAPHY PROGRAMS

Ocean Engineering Report No. 22

May, 1980

Department of Civil Engineering
University of Delaware
Newark, Delaware

LABORATORY DRIFT-VELOCITY DISTRIBUTION AT WAVE BREAKING POINT WITH SOME IMPLICATIONS TO SEDIMENT TRANSPORT PROCESSES

by

Tsuguo Sunamura, David Yang and Hsiang Wang

TECHNICAL REPORT NO. 5
OCEAN ENGINEERING
Supported by ONR Contract Number N00014-76-C-0342
ONR Geography Programs

May 1980

TABLE OF CONTENTS

LIST OF FIGURES

LIST OF FIGURES (CONTINUED)

LIST OF TABLES

LIST OF SYMBOLS

C	Wave celerity.
g	Gravitational acceleration.
h	Water depth.
H	Wave height.
k	Wave number.
L	Wavelength.
T	Wave Period.
U	Mean drift velocity.
$\bar{U}$	Depth-averaged mean drift velocity.
z	Vertical coordinate measuring from bottom.
κ	H_b/h_b
η	Water elevation.

Subscripts

b	Breaking condition.
o	Deep water condition.

ABSTRACT

Experiments were conducted in the laboratory to determine the drift velocity (mass transport velocity) at the breaking point on a beach with a slope of 1 to 15. Breaker types ranging from spilling to plunging were tested.

It was found that, irrespective of breaker types, the drift velocity is onshore near the surface and close to the bottom; in the main flow column, the drift velocity is always offshore. The vertical distribution of the drift velocity in the main water column is more uniform than that in the offshore region.

The influence of drift velocity on the sediment transport and beach profile changes is discussed.

I. INTRODUCTION

Drift-velocity in a wave field is the velocity of a mean current resulting from open orbital motions of water particles. It plays an important role in material transport in the nearshore zone and is also known as the mass transport velocity. Stokes (1847) was the first one who pointed out this property and treated the problem analytically for a channel of infinite length and constant depth. His solution, based upon classic second-order wave theory, results in a mean flow in the direction of wave propagation.

Longuet-Higgins (1953) treated the problem in a finite-length channel with due consideration of fluid viscosity in the surface and bottom boundary layers. His solution indicated that the drift velocity is in the direction of waves near the surface and the bottom but against the wave in the middle section. Later on, Huang (1970), Wang and Liang (1975), Mei, et al. (1972), and Dalrymple (1976), carried out further analytical studies, all of them dealt with finite channel of horizontal bottom. The drift velocity distributions obtained by them, except Dalrymple's, are all similar to that of Longuet-Higgins. Dalrymple's formulation was based on Dean's (1965) stream function theory and his solution was in the Eulerian sense as opposed to the Lagrangian drift velocity used by the other investigators.

Experimentally, Russell and Osorio (1958) measured drift velocity distribution in a horizontal finite-length channel. Bijker et al. (1974) investigated the influence of bottom slope on drift velocity. Most of their measurements were made before wave breaking with emphasis on

near-bottom flow. For the bottom drift velocity, they modified Longuet-Higgins' solution by the incorporation of shoaling effect. The theoretical values, however, are found to be considerably larger than those obtained in the experiments.

The present wave tank study concentrates the measurement of the drift velocity at the breaking point under different types of breaking waves on a rigid, plane beach, and describes some implications to sediment transport processes.

Two distinct types of breaking waves are usually seen on sloping beaches: plunging and spilling breakers. The difference in breaker types would probably influence the vertical drift-velocity profile at the breaking point, which would in turn control the sediment transport pattern across the surf zones. An attempt is made here to clarify the drift velocity patterns under these breakers.

For the convenience of reference, we define (1) the breaking point as a starting point of wave breaking, which is characterized by the existence of maximum height of waves, usually showing the initiation of bubble and foam formation; and (2) the plunging point as a point where the shape of breaking waves completely disintegrates when their crest impinges against water (see Fig. 1). The drift velocity distributions are largely measured within these limits.

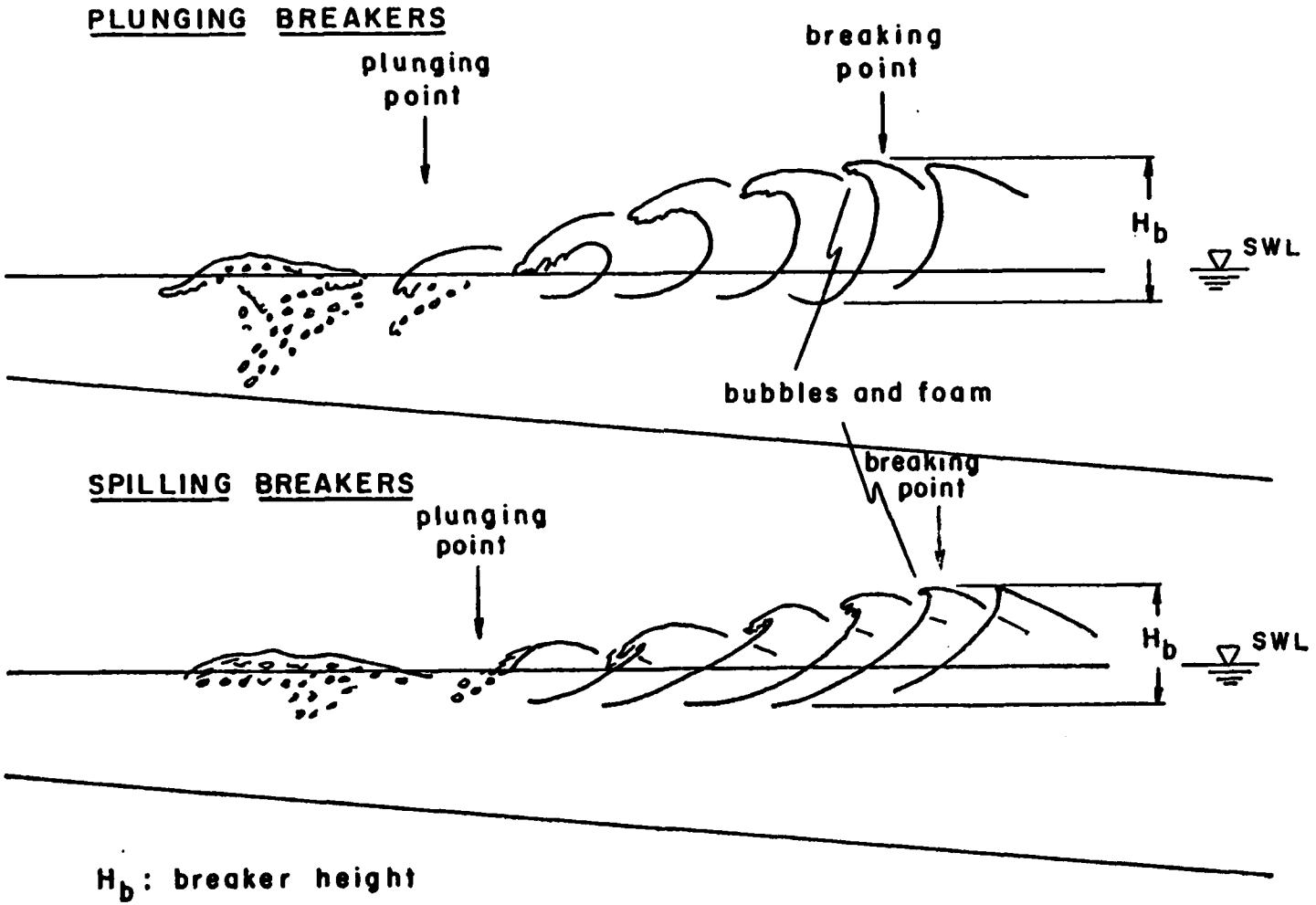

Fig. 1. Definition of breaking wave.

II. LABORATORY EXPERIMENT

II-1. Experimentation

A steel-made wave tank, with a glass-made observation window on one side, was used; the tank, 20 m long, 0.6 m wide, and 1.3 m high, was equipped with a Scotch Yoke type monochromatic wave generator. A 1/15 plane beach, made of a plywood coated with black paint, was placed with the tip located at a distance of 8 m from the wave paddle.

Seven runs of experiments were conducted with different breaker types: three of them were plunging, two were spilling, and the remaining two were transition-type breakers (Table 1). Input wave characteristics were recorded by a capacitance type wave gauge installed at a place of constant water depth.

In order to trace wave-induced water movement near the breaking point, neutrally buoyant, polystyrene beads were used. They were yellow-colored with a diameter of approximately 2 mm. Not all the beads had exactly the same density as the water which actually resulted in a more uniform vertical distribution of beads in the water column.

Figure 2 illustrates apparatus setup at a measuring section which was covered with a wooden board having a slit (9 cm x 66 cm); the light of three lamps (500 W each) over the board illuminated the measuring section (through the slit). The neutrally buoyant artificial particles were mixed with water in a tracer feeder made of a transparent plastic tube with an outer diameter of 1 cm. One tapered end of the feeder was placed on the bottom under the breaking point, while the other end was

TABLE 1

LABORATORY RESULTS

Run	MEASURED DATA					CALCULATED DATA							Breaker*** Type
	T (sec)	H (cm)	H_b (cm)	h_b (cm)	$\bar{U}$ (cm/sec)	L_o (cm)	H_o* (cm)	H_o/L_o	H/L_oS^{2}**	κ (H_b/h_b)	κ^2	$\bar{U}/\sqrt{gh_b}$	
1	1.89	12.5	16.5	17.1	4.8	557	12.9	0.023	5.1	0.96	0.92	0.037	PL
2	1.65	13.6	16.5	18.3	3.1	425	14.5	0.034	7.6	0.90	0.81	0.023	PL
3	1.47	11.9	14.5	18.6	2.5	337	12.9	0.038	8.4	0.78	0.61	0.019	TR
4	1.33	11.7	14.0	18.3	2.6	276	12.8	0.046	10.2	0.77	0.59	0.019	SP
5	1.56	8.4	12.5	13.7	2.8	380	9.04	0.024	5.3	0.91	0.83	0.024	PL
6	1.34	9.0	11.5	13.1	2.3	280	9.85	0.35	7.8	0.88	0.77	0.020	TR
7	1.00	8.0	9.5	12.1	1.3	156	8.56	0.035	12.2	0.79	0.62	0.013	SP

*$H/H_o = \left[\left(1 + \frac{2kh}{\sinh 2kh}\right)\tanh kh\right]^{-1/2}$, h = 40 cm.

Assuming no reflection and no friction-percolation loss

**S = Slope of plane beach = 1/15 for this experiment; Galvin (1968).

***PL = Plunging; TR = Transition; SP = Spilling

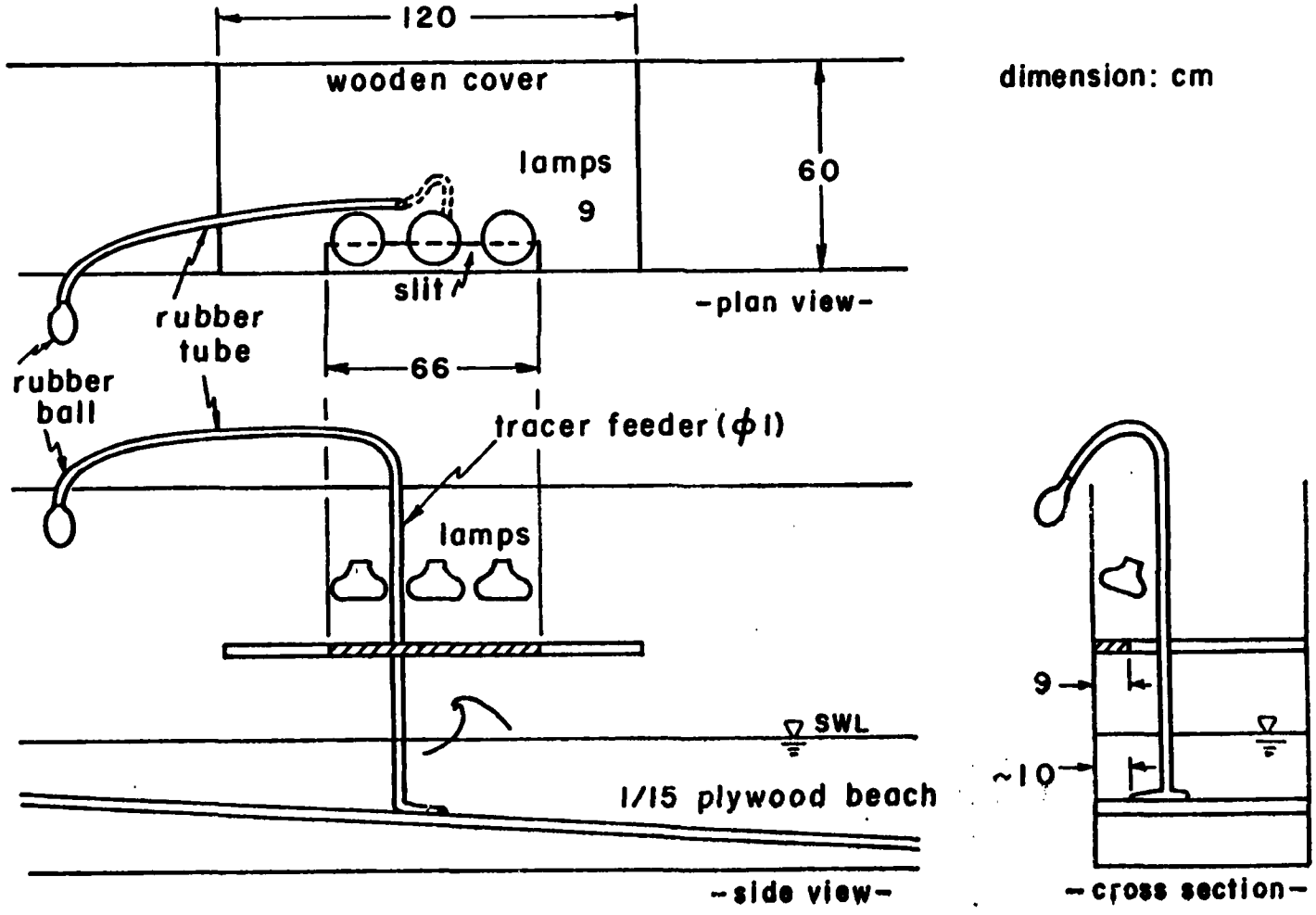

Fig. 2. Schematic diagram showing measuring apparatus.

connected to a rubber ball by a rubber tube. By squeezing the ball during wave action, many tracers were ejected from the feeder tip into water-in-motion; some tracers, slightly lighter than water, went up slowly; so that almost uniform tracer-distribution around the breaking point was attained in a few wave cycles after the ejection (Photo 1).

The movement of the tracers was filmed, over 10 consecutive wave cycles for each run, by using a 16-mm movie camera (Bolex, H-16, EBM Electric) operated at a speed of 25 frames/sec. Color films (Kodachrome 40) were used. A 100-mm telephoto lens was applied to reduce the parallax.

II-2. Data Analysis

Trajectories of beads (Photos 2 and 3) were traced, as many as practical, from the films with the aid of a film analyzer (L-W International, Model 224 A). Examples of trajectory diagrams are shown in Fig. 3. Greater turbulence caused by water-mass impinging at the plunging point, particularly in the case of plunging breakers of larger heights, affected the two-dimensionality of the flow field in the vicinity of the breaking point; this influenced the movement of the tracers. Consequently, long-term trajectory tracing was difficult in the plunging breaker cases (compare Figs. 3a and 3b).

Figure 4 shows a definition of mean drift velocity, U, at a point, $(\frac{x}{2}, \frac{y}{2})$:

$$U = \frac{a + b}{2T}$$

Photo 1

Uniformly Distributed Tracers After a Few Wave Cycles.

Photo 2

Trajectories of Beads During Advancing Wave Cycle.

Photo 3

Trajectories of Beads During Receding Wave Cycle.

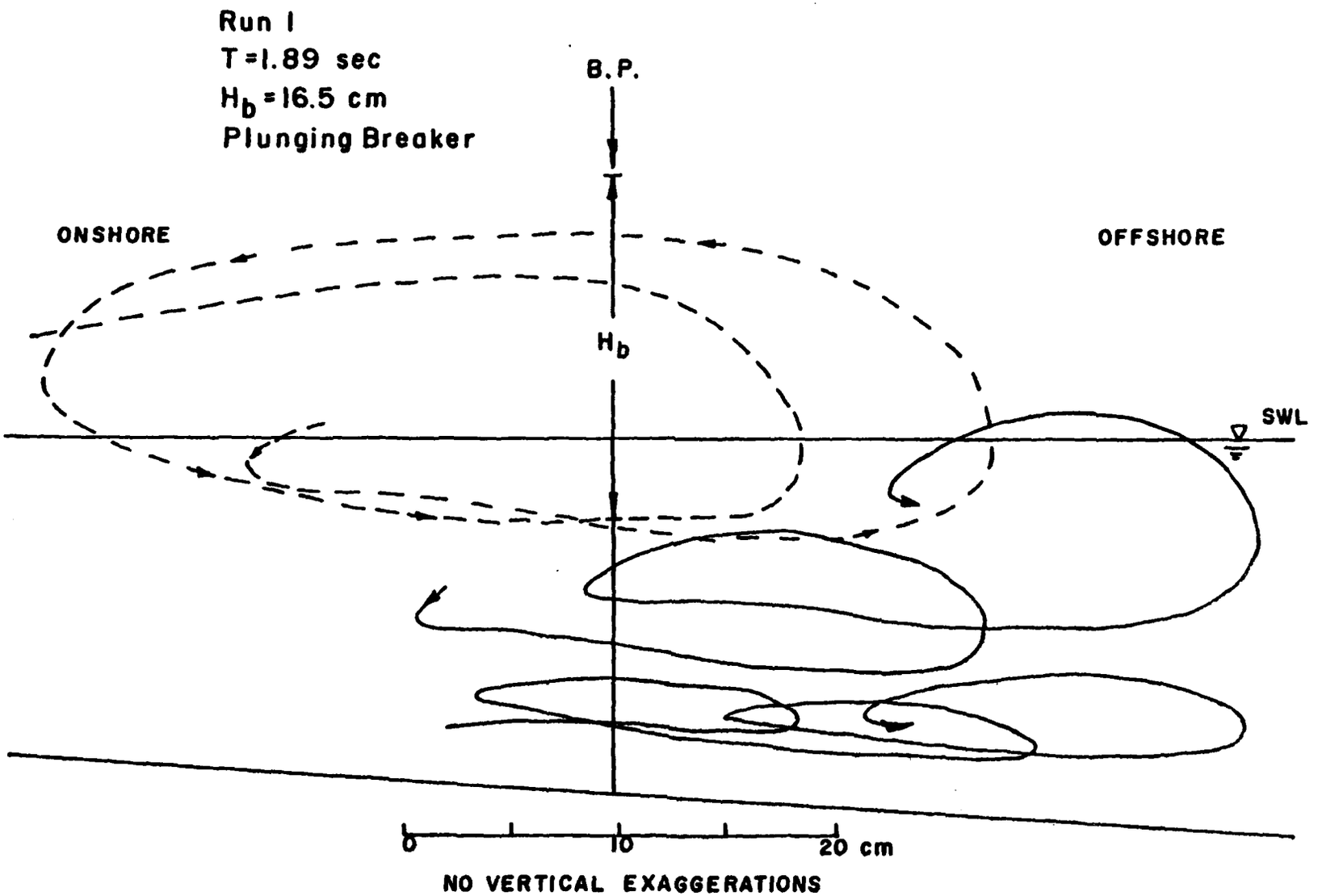

Fig. 3a. Some of tracer trajectories (Run 1].

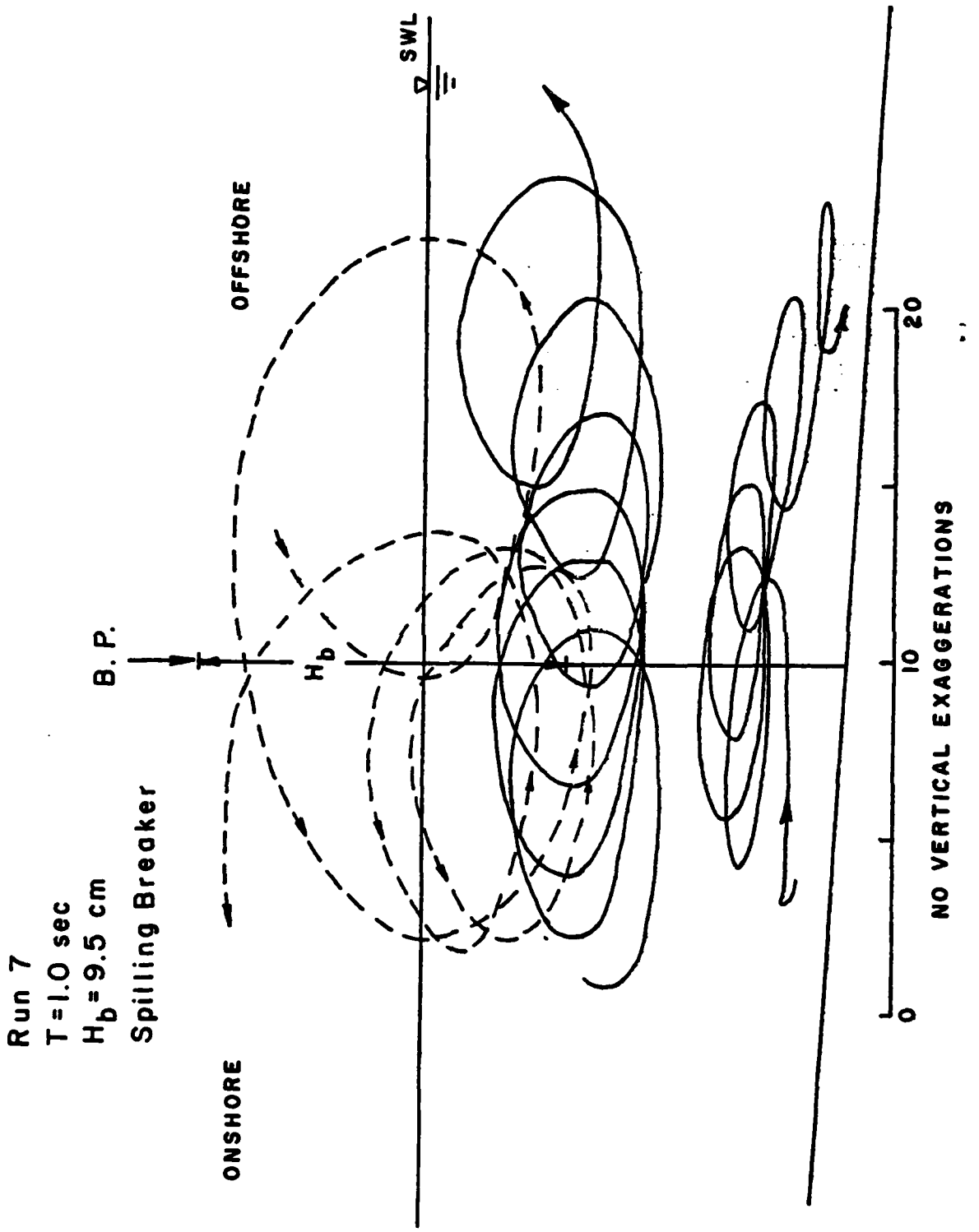

Fig. 3b. Some of tracer trajectories (Run 7).

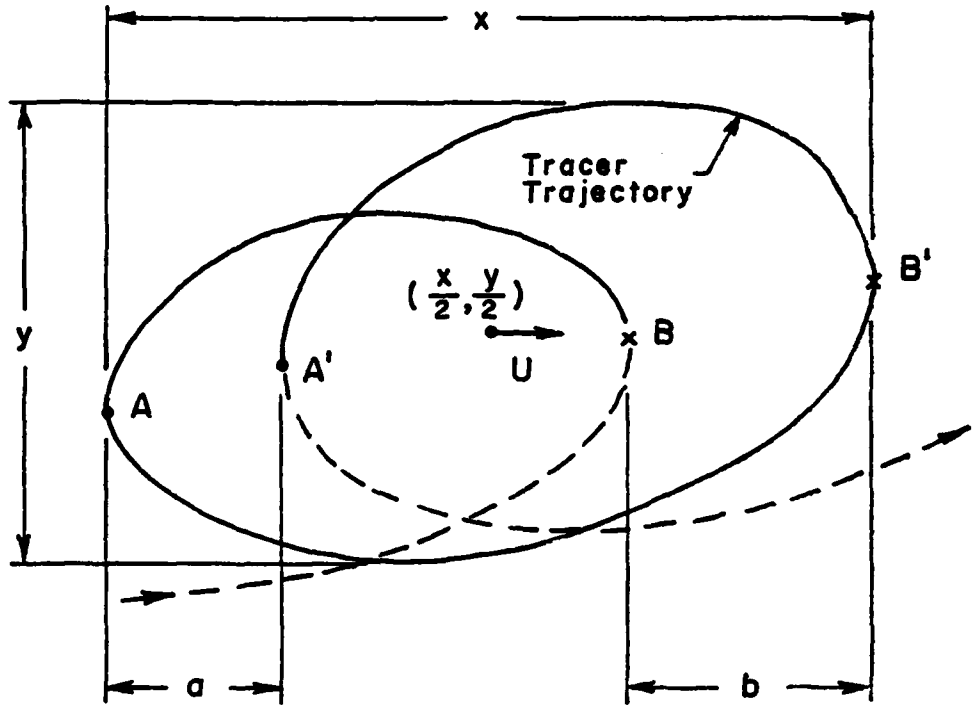

Fig. 4. Definition of mean drift velocity, U.

where T is wave period, a and b are the displacements of a tracer, measured with positive values in the offshore direction; and x and y are horizontal and vertical dimensions of the trajectory under consideration, respectively. Since the mean drift velocity, thus obtained from the trajectory diagrams, showed considerable spatial scatter (see Fig. 5, as an example), local averaging was done by grouping the data as demonstrated by dashed closures in Fig. 5; some ambiguity remained in the selection of averaging areas.

II-3. Results

On the basis of the locally averaged values, isolines were drawn to indicate drift-velocity distribution near the breaking point; the result is shown in Fig. 6, in which offshore drift is chosen as positive.

The lack of data points near the bottom was partially due to the difficulty of differentiating the tracers crowded in the vicinity of the bottom. The film analyses showed that there always exists a thin bottom layer having onshore drift velocity, irrespective of breaker types; this layer is about 1 cm or less in depth, although the exact determination was not possible. The bottom layer in Fig. 6 was drawn with this approximate depth.

A wide mid-layer shows offshore mass transport (Fig. 6). Since continuity has to be satisfied, onshore mass transport must exist near the water surface to balance the net offshore flow in the water column, i.e., the mid-layer offshore discharge minus the bottom-layer onshore

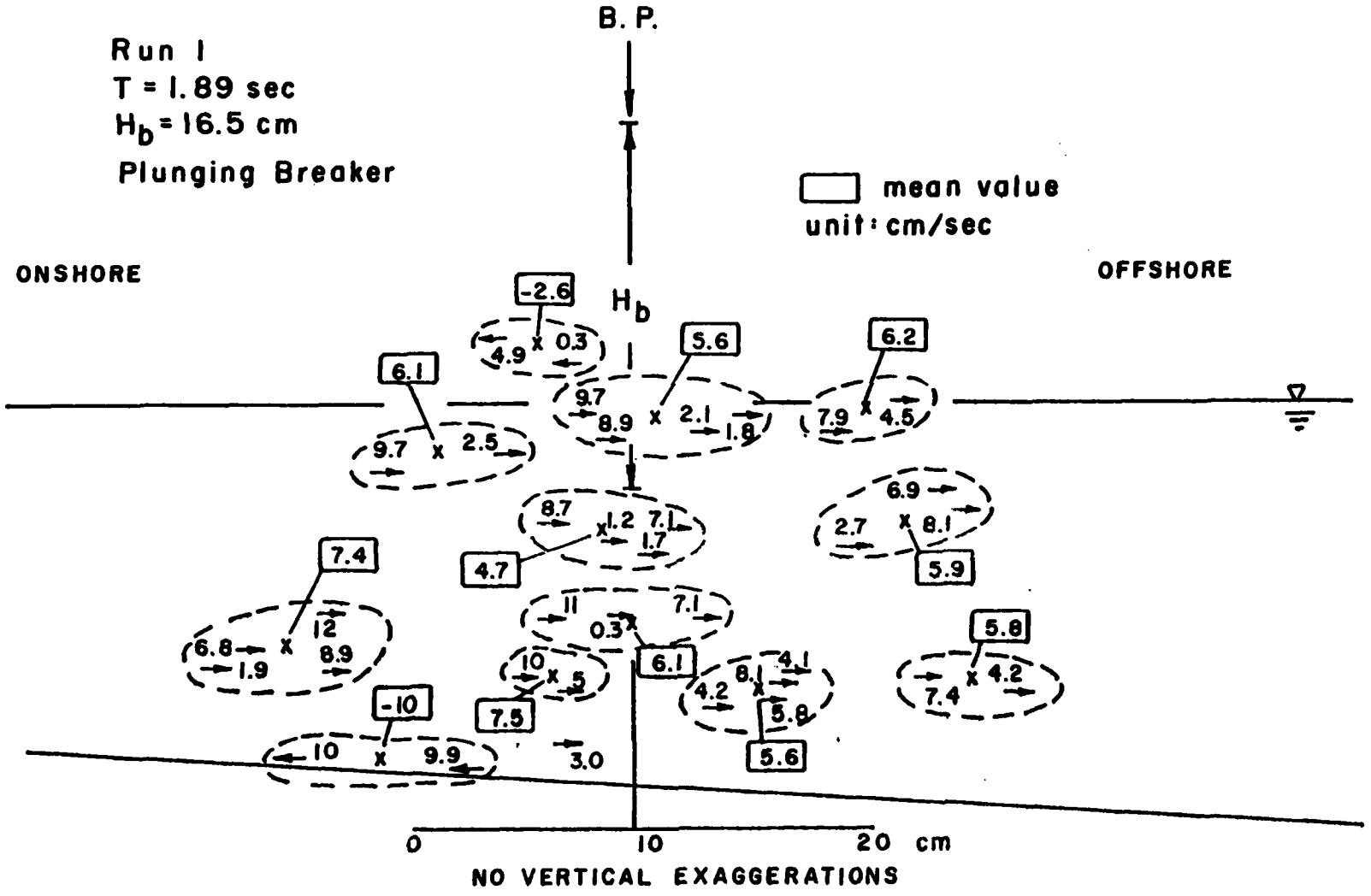

Fig. 5. Areal distributions of drift velocities and of locally averaged values.

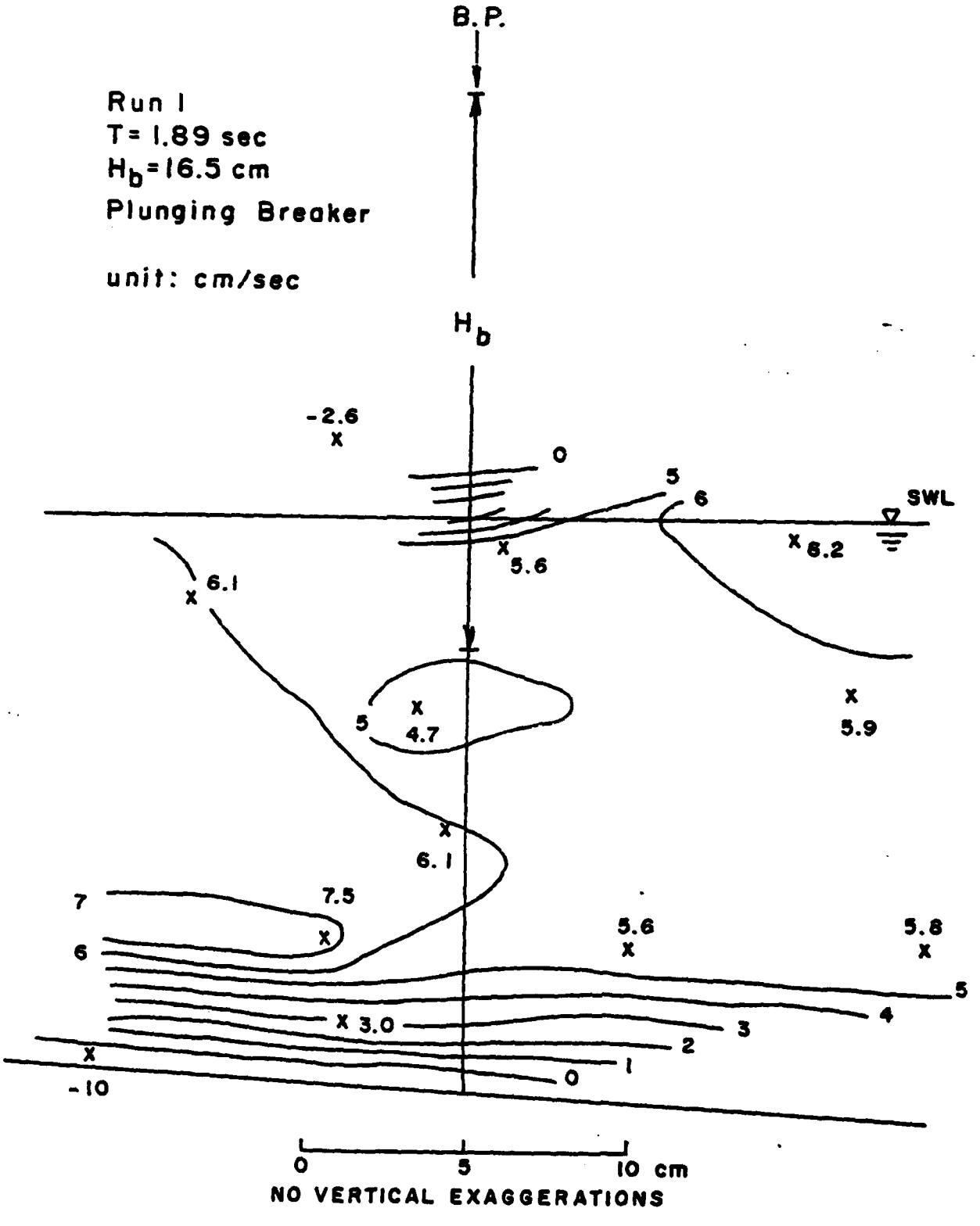

Fig. 6a. Drift-velocity distribution around the breaking point.

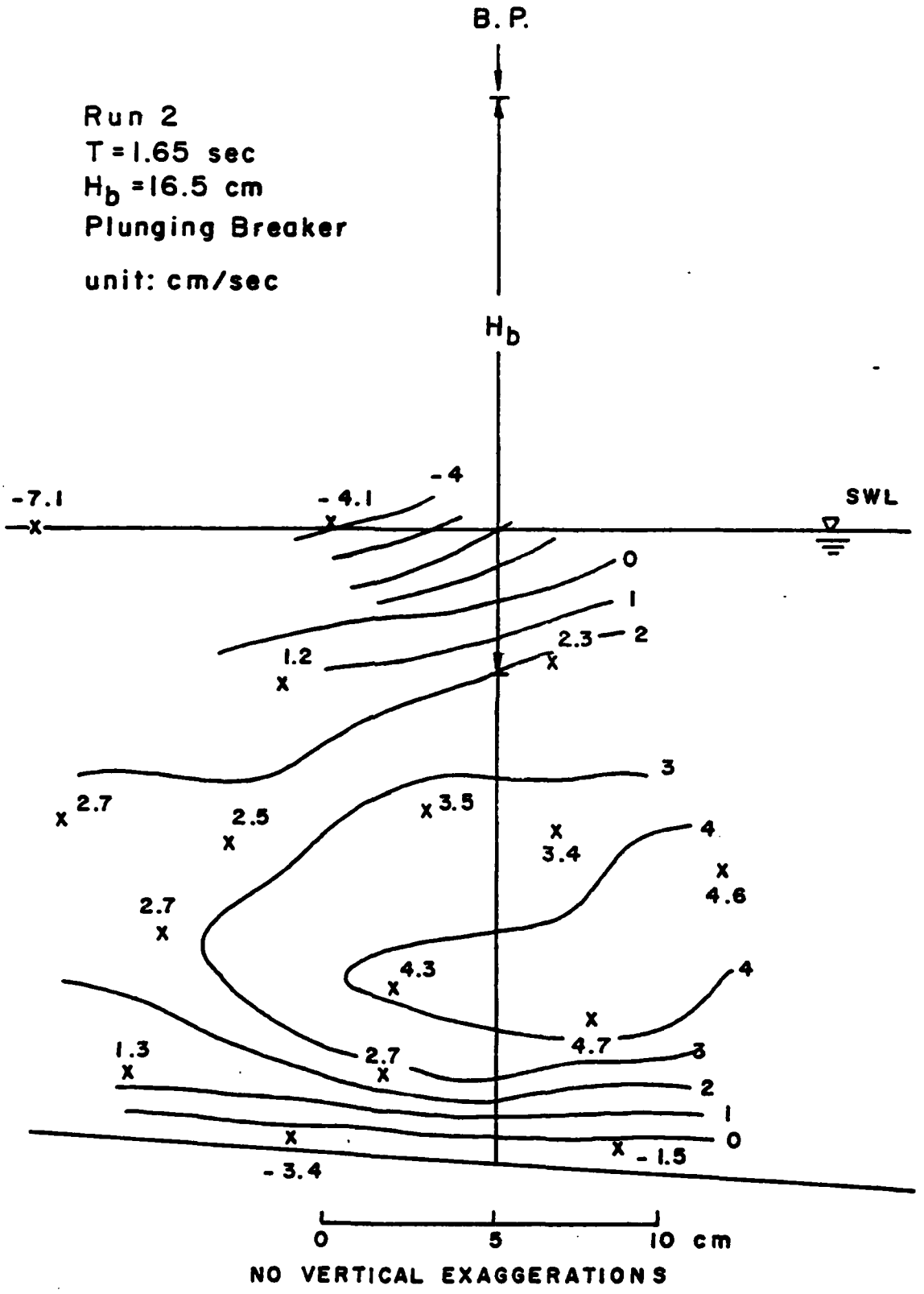

Fig. 6b. Drift-velocity distribution around the breaking point.

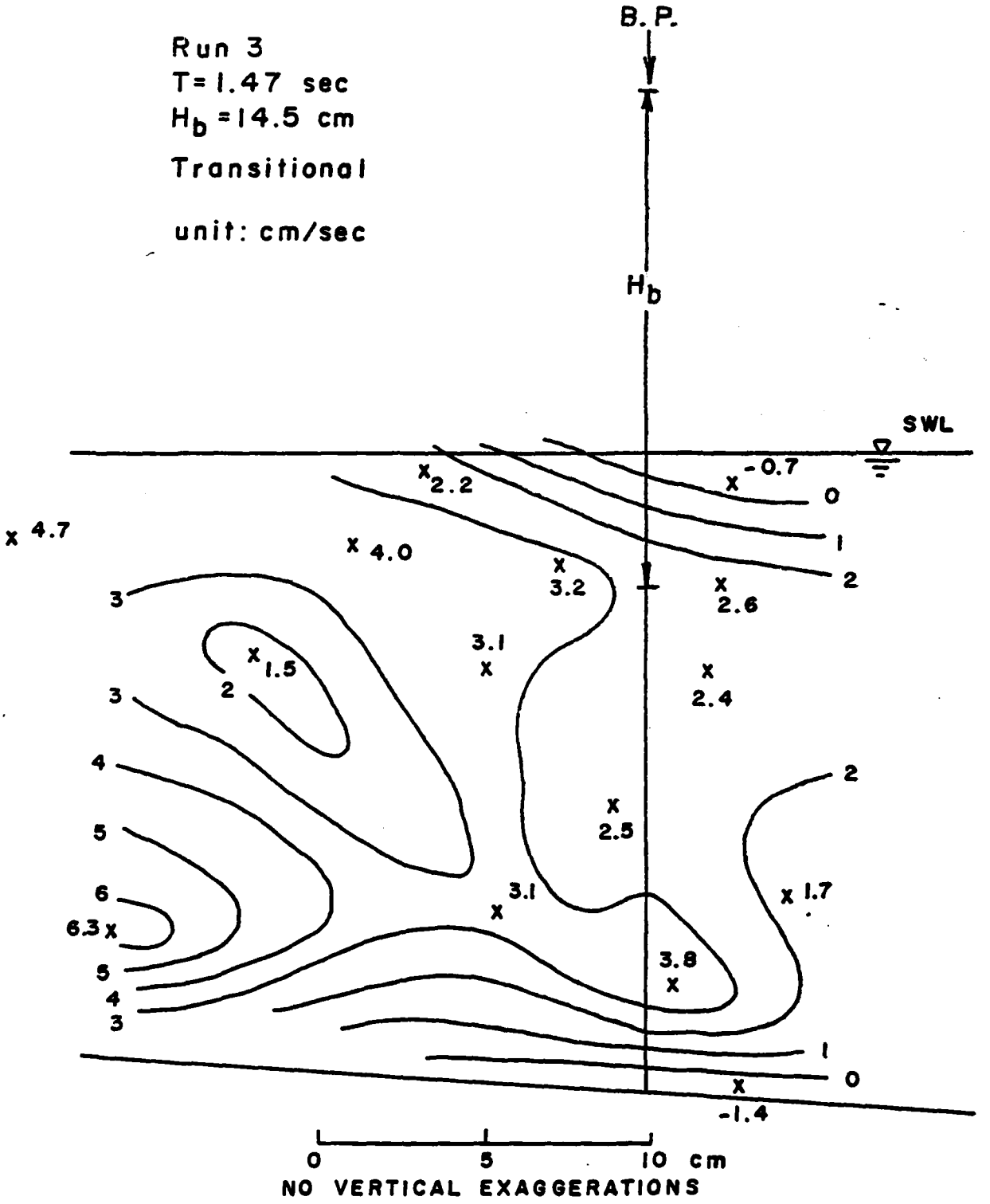

Fig. 6c. Drift-velocity distribution around the breaking point.

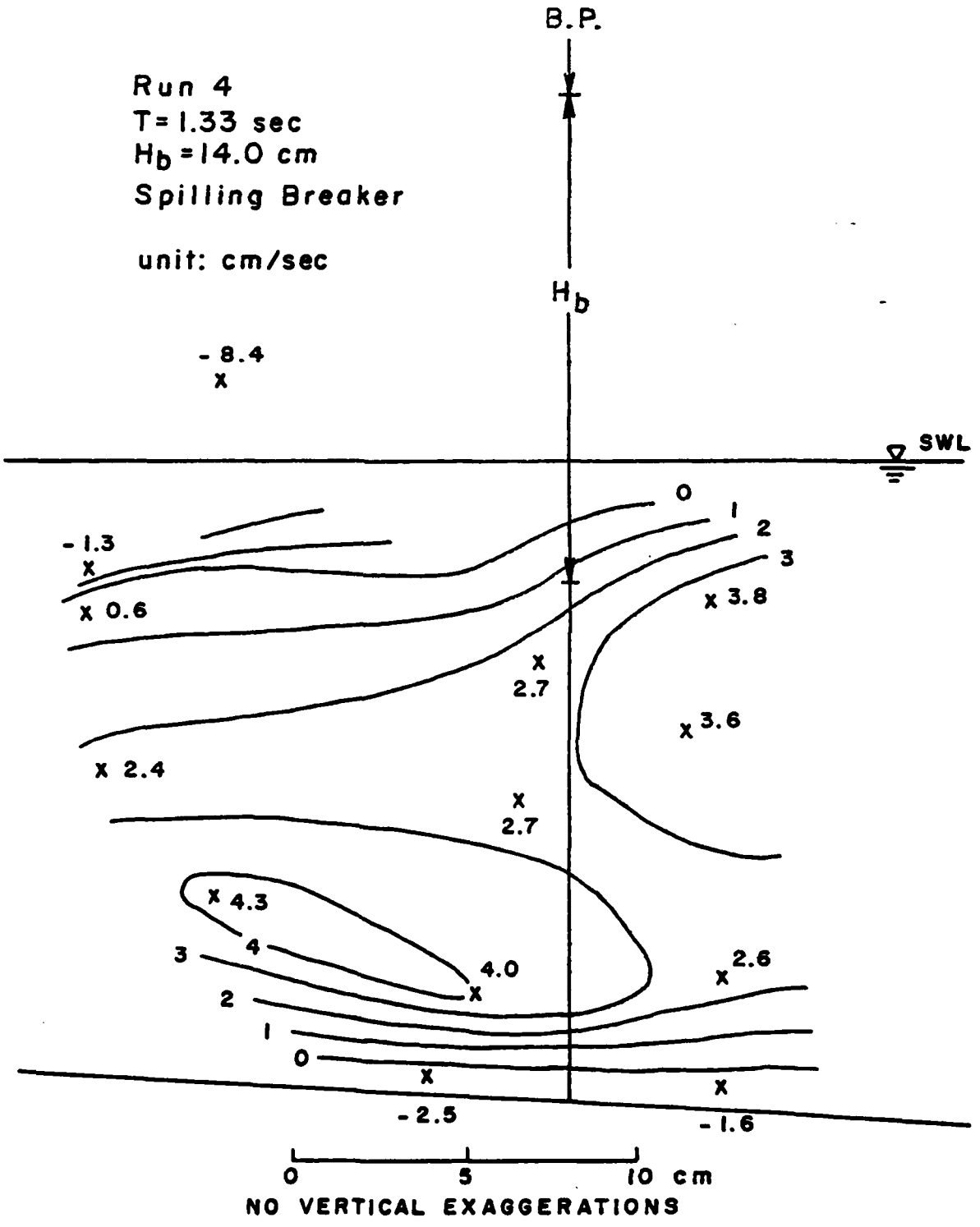

Fig. 6d. Drift-velocity distribution around the breaking point.

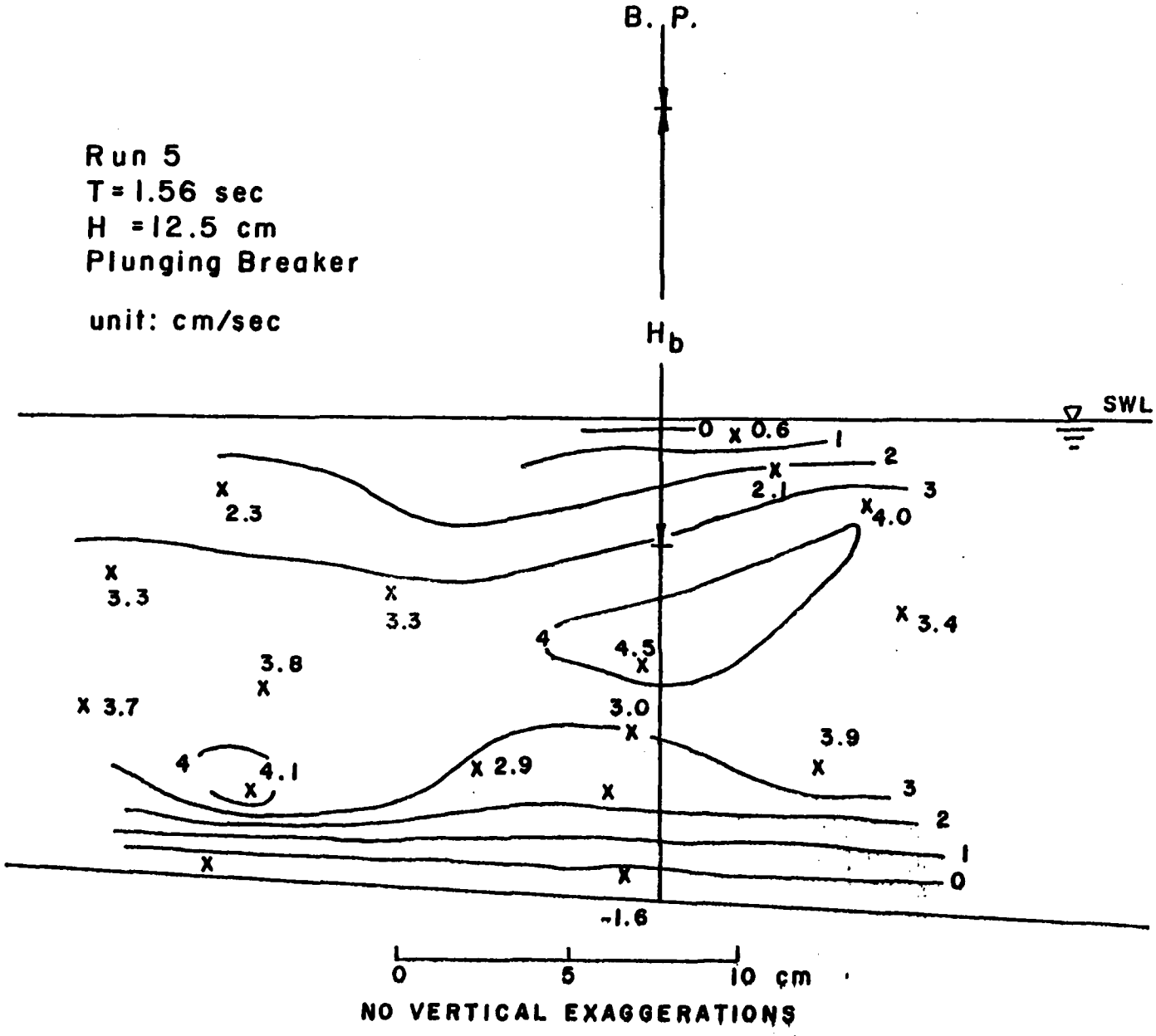

Fig. 6e. Drift-velocity distribution around the breaking point.

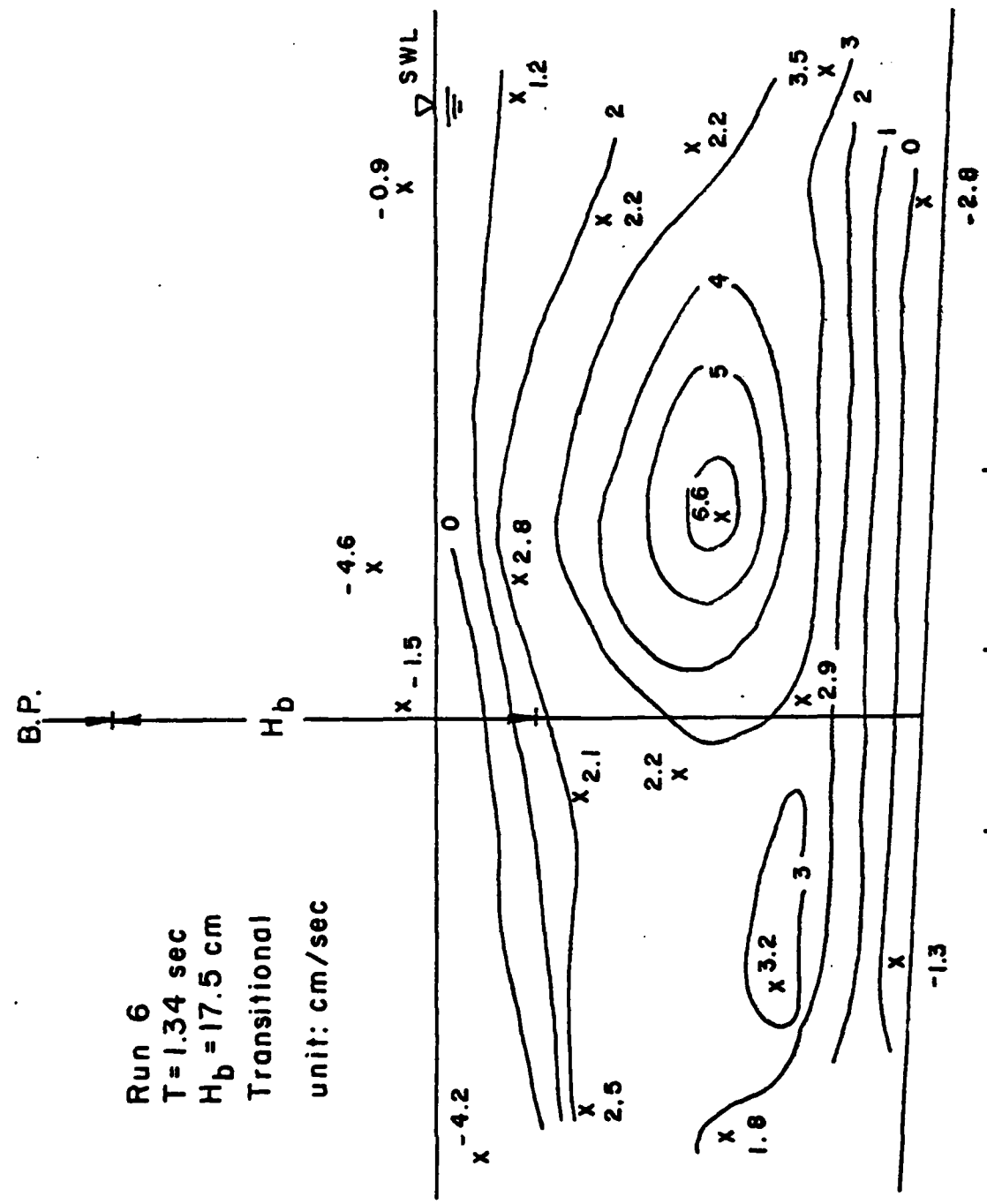

Fig. 6f. Drift-velocity distribution around the breaking point,

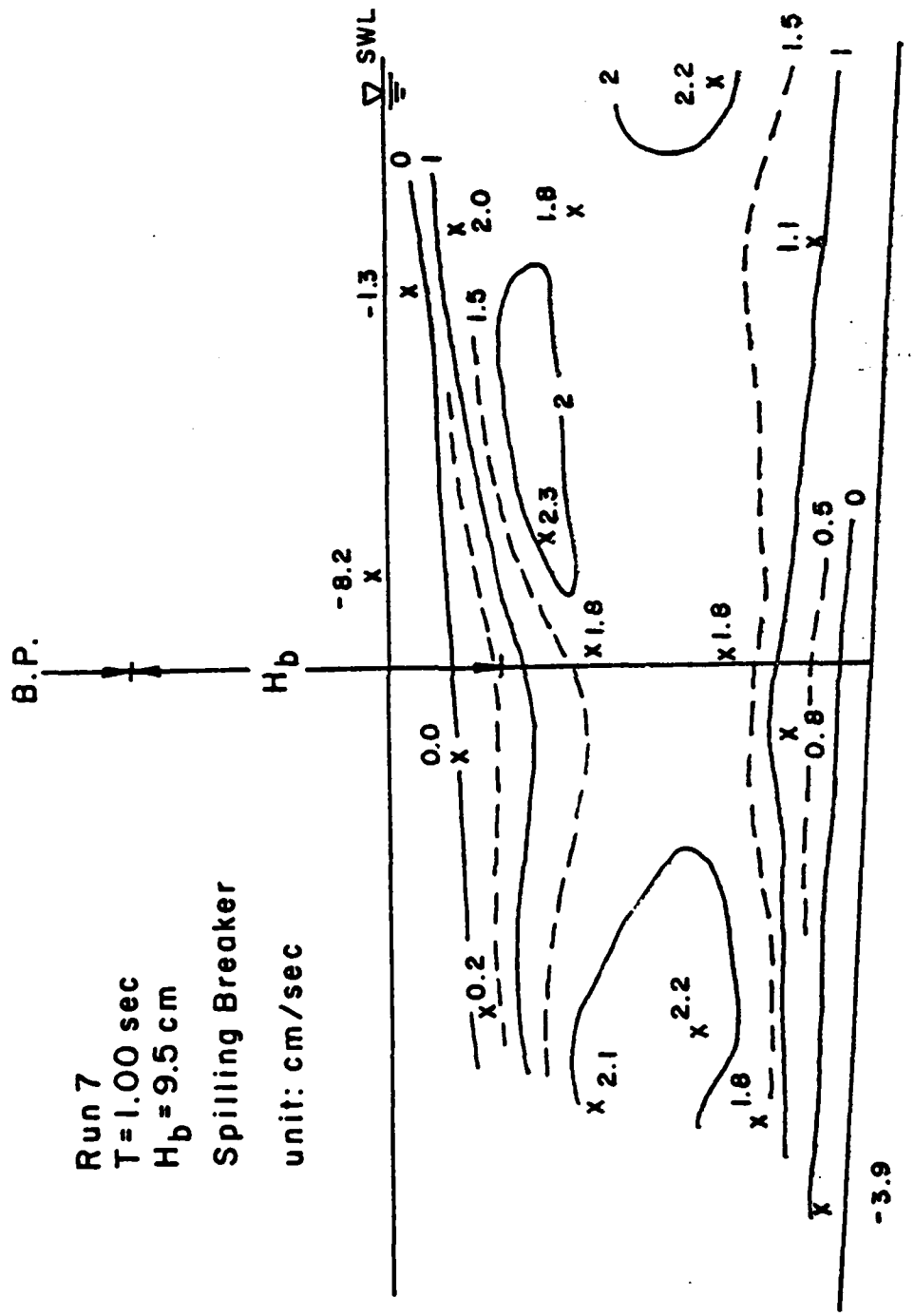

Fig. 6g. Drift-velocity distribution around the breaking point,

discharge. Adequate measurement of the upper-layer onshore mass movement velocity was not practical by the tracer method because a large quantity of air bubbles formed at the initial stage of wave breaking.

Figure 7 shows the vertical distributions of drift velocity at the breaking point. The values were based on isolines intersecting with a vertical plane at the breaking point. Again, quantitative determination of the onshore velocity on the bottom could not be made because of the inaccurate measurement. The offshore drift velocity in the interior region, in general, shows a fairly uniform vertical distribution. There seems to be little difference in the offshore drift velocity profile between plunging and spilling breakers: the former might have a slight bulge in the lower or middle part of the profile, while the latter has none, as schematically drawn in Fig. 8.

III. DATA INTERPRETATIONS

Vertical distribution of drift velocity at the breaking point as obtained in the present experiment is qualitatively similar to that in the offshore zone on a uniformly sloping smooth bottom (Bijker et al. 1974) and, to an extent, similar on a horizontal bottom (Russel and Osorio 1958) (Fig. 9). They all have onshore drift in the surface and bottom layers and offshore flow in the interior layer. The shapes of the vertical distribution are, however, different. Bijker's measurements, for instance, showed rather uniform vertical distribution in the offshore region but became progressively more non-uniform towards the shoreline. The present results, on the other hand, yielded rather uniform distributions at the breaking point.

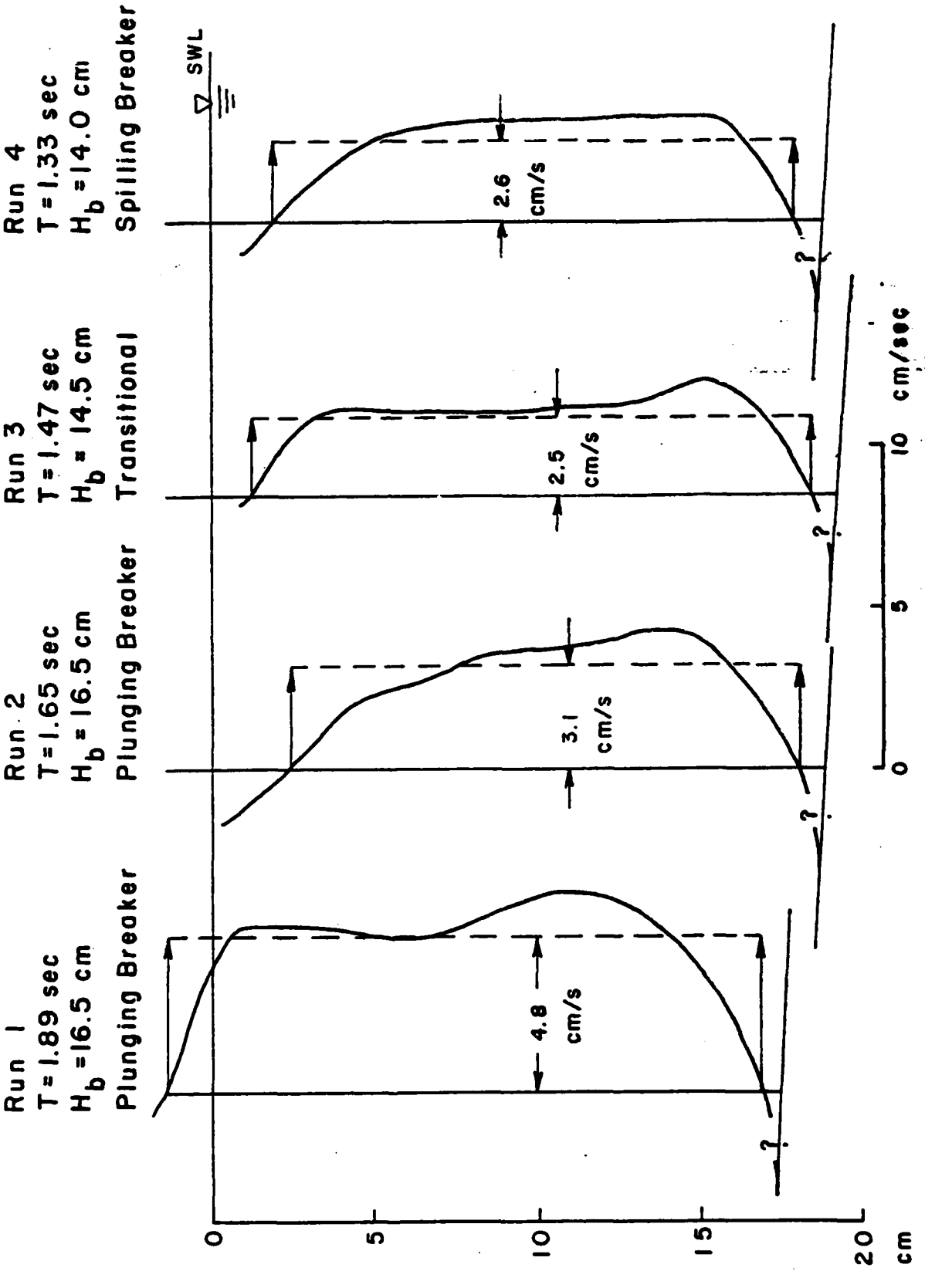

Fig. 7a. Vertical distributions of drift velocity at the breaking point.

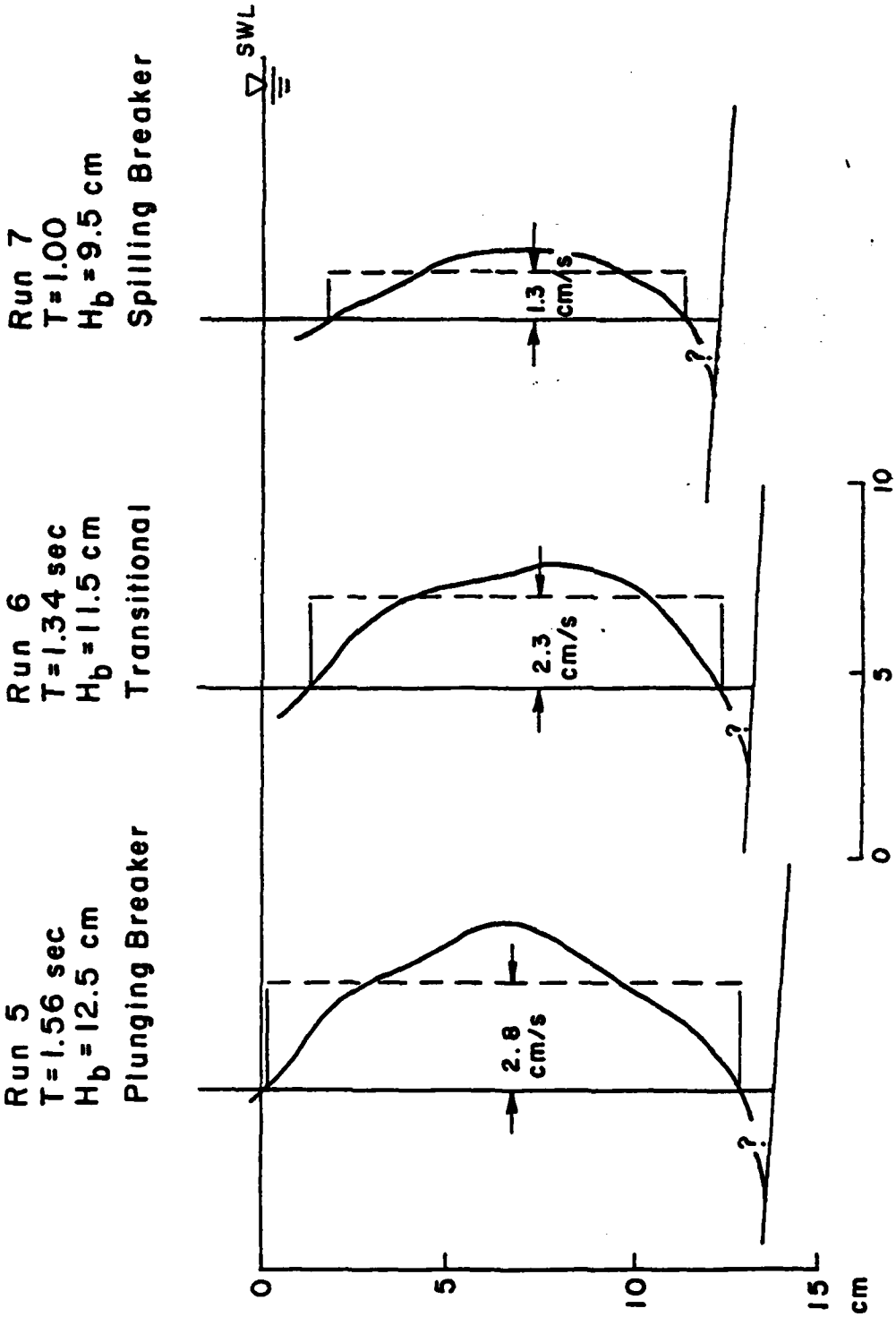

Fig. 7b. Vertical distributions of drift velocity at the breaking point.

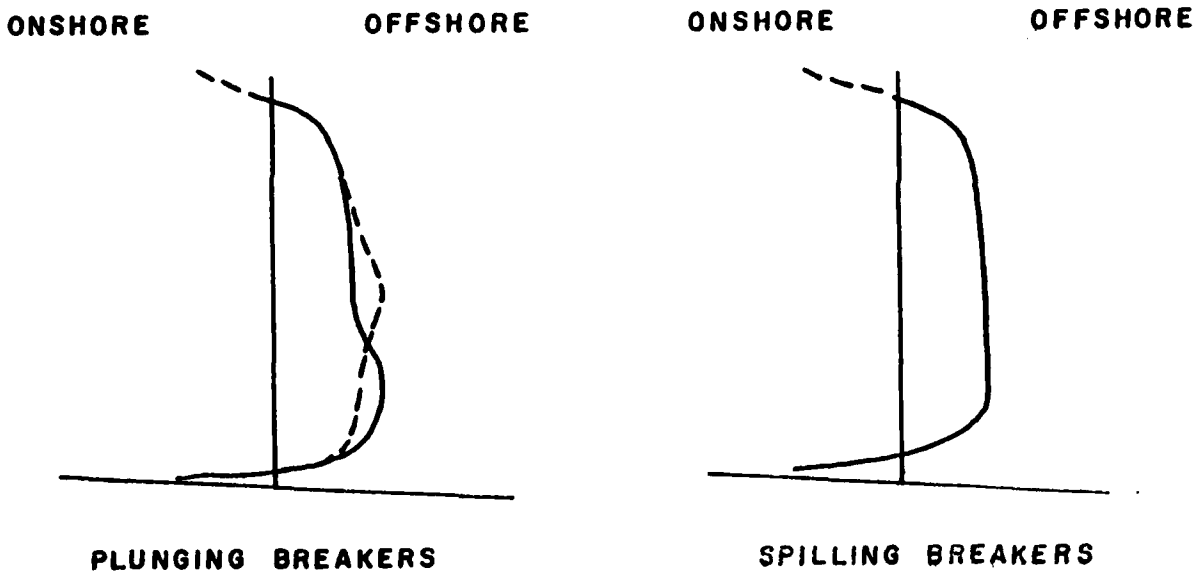

Fig. 8. Possible offshore drift-velocity profiles at the breaking point.

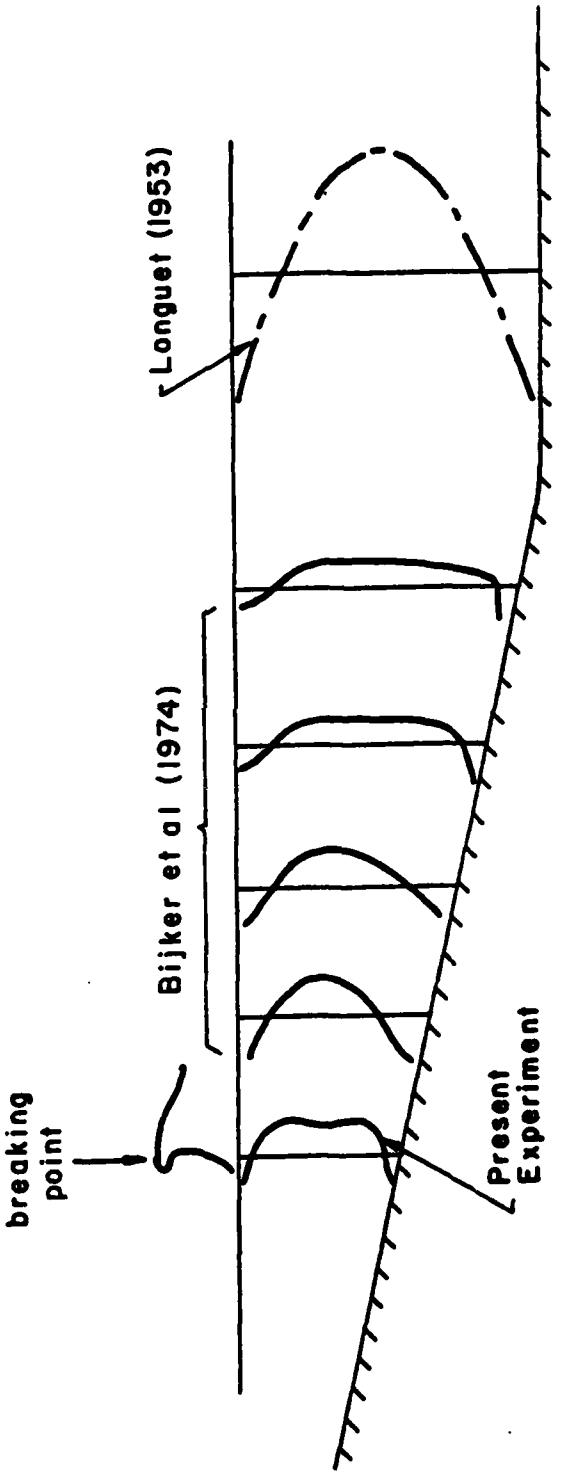

Fig. 9. Vertical distribution of drift velocity on a sloping beach.

In the above equation, $\frac{1}{2}\left(\frac{\pi H}{L}\right)^2 \frac{C}{\sinh^2 2\pi\left(\frac{h}{L}\right)}$ dictates the mean strength and f(L,h,z) is the shape function. If Eq. (1) is valid up to the breaking point, we have

$$U_b(z) = \frac{1}{2}\left(\frac{\pi H_b^2}{L_b}\right)^2 \frac{C}{\sinh^2 \frac{2\pi h_b}{L_b}} f(L_b, h_b, z) \qquad (2)$$

The subscript "b" refers to breaking condition. Furthermore, in shallow water the following approximations can be applied:

$$\left.\begin{aligned} C_b &= \sqrt{gh_b} \\ \sinh \frac{2\pi h_b}{L_b} &= \frac{2\pi h_b}{L_b} \end{aligned}\right\} \qquad (3)$$

Substituting Eq. (3) into Eq. (2) leads to:

$$U_b(z) = \frac{1}{8} \frac{H_b^2}{h_b^2} \sqrt{gh_b}\, f(L_b, h_b, z) \qquad (4)$$

The mean offshore drift velocity at the breaking point, $\overline{U_b}$, is defined as

$$\overline{U_b} = \frac{1}{h_2 - h_1} \int_{h_1}^{h_2} U_b(z)\, dz$$

where h_2 and h_1 are the upper and lower limits of the offshore flow, respectively. Therefore, integrating Eq. (4) yields the following non-dimensional drift velocity:

When a wave train proceeds on a sloping beach, it shoals as well as feels the bottom. Prior to breaking, the shoaling effect causes more mass transport in the wave propagation direction; this added onshore transport probably concentrates in the surface layer as shown by Dalrymple (1976). The bottom effect retards the return flow. Therefore, the combined effects results in an offshore flow bulged in the interior region. When a wave experiences breaking, a great amount of turbulence is generated within a short distance which smoothes the vertical velocity distribution much the same as the eddy viscosity effect on the longshore current distribution. Thus, at the breaking point, the vertical distribution of the drift velocity becomes much uniform.

To estimate the mean offshore drift velocity at the breaking point, we begin here by considering Longuet-Higgins' solution for the interior region in a channel of constant depth which is

$$U(z) = \frac{1}{2}\left(\frac{\pi H}{L}\right)^2 \frac{C}{\sinh^2 2\pi\left(\frac{h}{L}\right)} f(L,h,z) \qquad (1)$$

where

$$f(L,h,z) = \frac{1}{2}\left\{ \begin{array}{l} 2\cosh 4\pi\left(\frac{h+z}{L}\right) + 3 + 2\pi\left(\frac{h}{L}\right)\left[3\left(\frac{z}{h}\right)^2 + 4\left(\frac{z}{h}\right) + 1\right] + \sinh 2\pi\frac{h}{L} \\ + 3\left[\frac{\sinh 4\pi\left(\frac{h}{L}\right)}{4\pi\left(\frac{h}{L}\right)} + \frac{3}{2}\right]\left[\left(\frac{z}{h}\right)^2 - 1\right] \end{array} \right.$$

with $U(z)$ is the mean drift velocity at depth z.

H is the wave height;

L is the wavelength, and

h is the water depth.

$$\frac{\overline{U_b}}{\sqrt{gh_b}} = A\kappa^2 \qquad (5)$$

where $\kappa = H_b/h_b$

and $$A = \frac{1}{8(h_2 - h_1)} \int_{h_1}^{h_2} f(L_b, h_b, z)\,dz$$

In the above derivation, the shoaling effects as well as the bottom friction is ignored. If these effects are to be included in the coefficient, no analytical expression is available at present; the value of "A" has to be determined experimentally. The data of the depth-averaged mean offshore drift is plotted against κ^2 in Fig. 10. The actual data are summarized in Table 1. If the coefficient A is computed on the basis of Longuet Higgins' solution applied to the breaking depth, the best fit should be A = 0.029. This line is plotted in the same figure for comparison.

IV. EFFECTS ON SEDIMENT TRANSPORT PROCESSES

As is shown in the previous sections, the vertical distribution of drift velocity in the offshore zone has similar profiles up to the breaking point, with onshore net flow near the bottom, and offshore flow in the interior region.

If the bottom is made of movable material like sands, the turbulence caused by breaking waves, especially near the plunging point, sets the material in suspension. The finer the sediments are, the longer and higher they remain in suspension. The once suspended sediments are easily transported offshore, if they are captured by the mid-layer

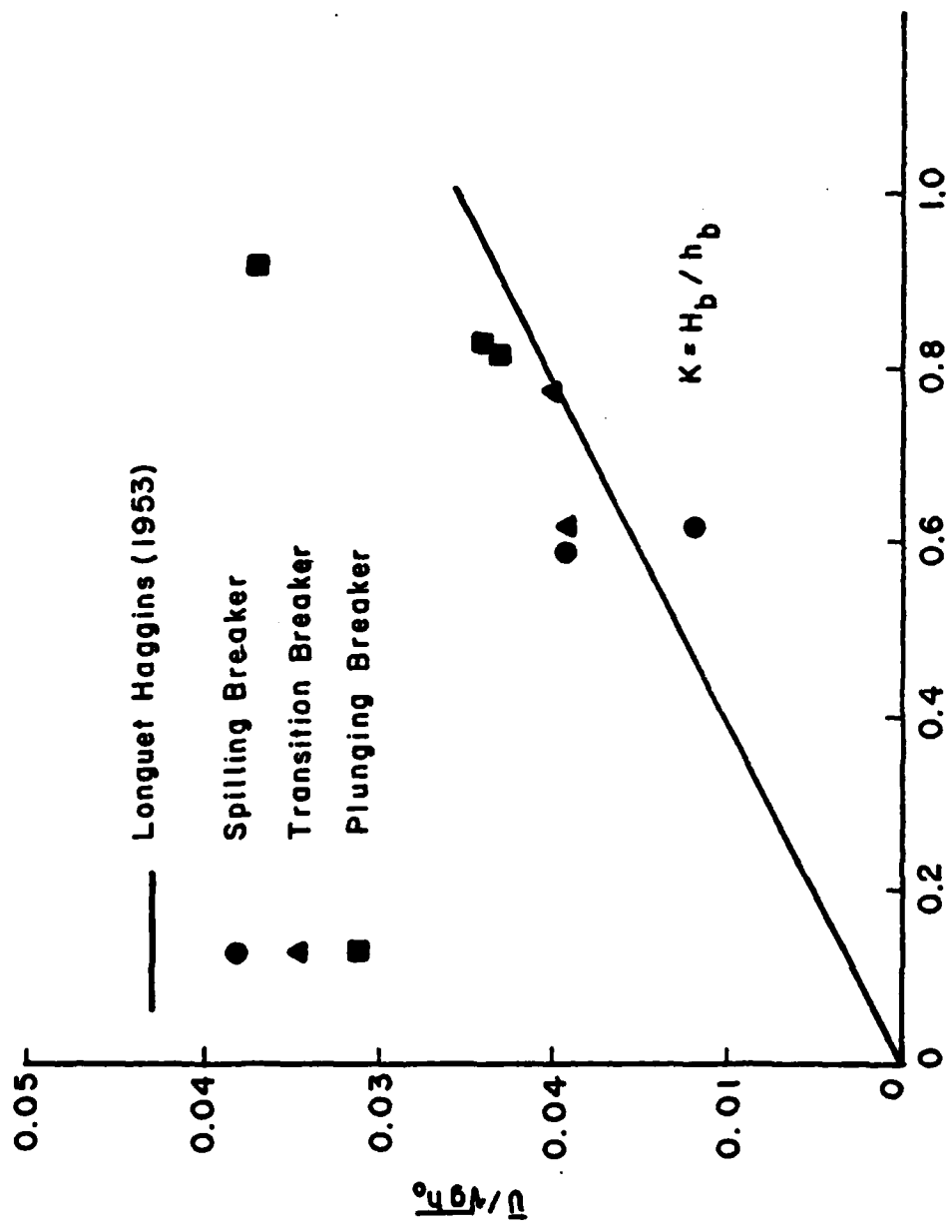

Fig. 10. Depth-averaged mean drift velocity vs. K^2.

offshore flow at the breaking point. The offshore transported material, beyond the breaking point, is soon fallen down to the bottom due to (1) the effect of gravity and (2) the abrupt decrease of turbulence, which is the major mechanism of keeping the sediments in suspension. Simultaneous to this offshore transport in the mid-layer, sands on the bottom, both near the breaking point and in the offshore zone, are moving onshore due to the bottom onshore flow. Once the sands, transported offshore in the mode of suspension from the surf zone, touched the bottom, they might be carried back onshore to the surf zone.

In this onshore/offshore sediment transport process, the resulting bottom topography depends on the net sand discharge near the breaking point. If the onshore discharge is larger than the offshore one, then a beach is characterized by the surf-zone sand-accumulation, which forms a bar under certain conditions (A in Fig. 11) or a step under other circumstances (B in Fig. 11). One laboratory example of the former case is illustrated in Fig. 12: plunging breakers were acted on an 1/10 initial beach made of 0.7 mm sand; no sand ripples were formed on the bottom; the great turbulence of water, caused near the plunging point, scoured the bottom to form a trough giving rise to sediment suspension; some of the suspended sand was transported offshore, but was soon deposited on the bottom; this newly arrived material, together with the initial material in the offshore zone, is carried onshore as bed-load. These materials transported onshore build a bar inside the breaking point. A possible pattern of sediment transportation of this case is schematically shown in Fig. 13.

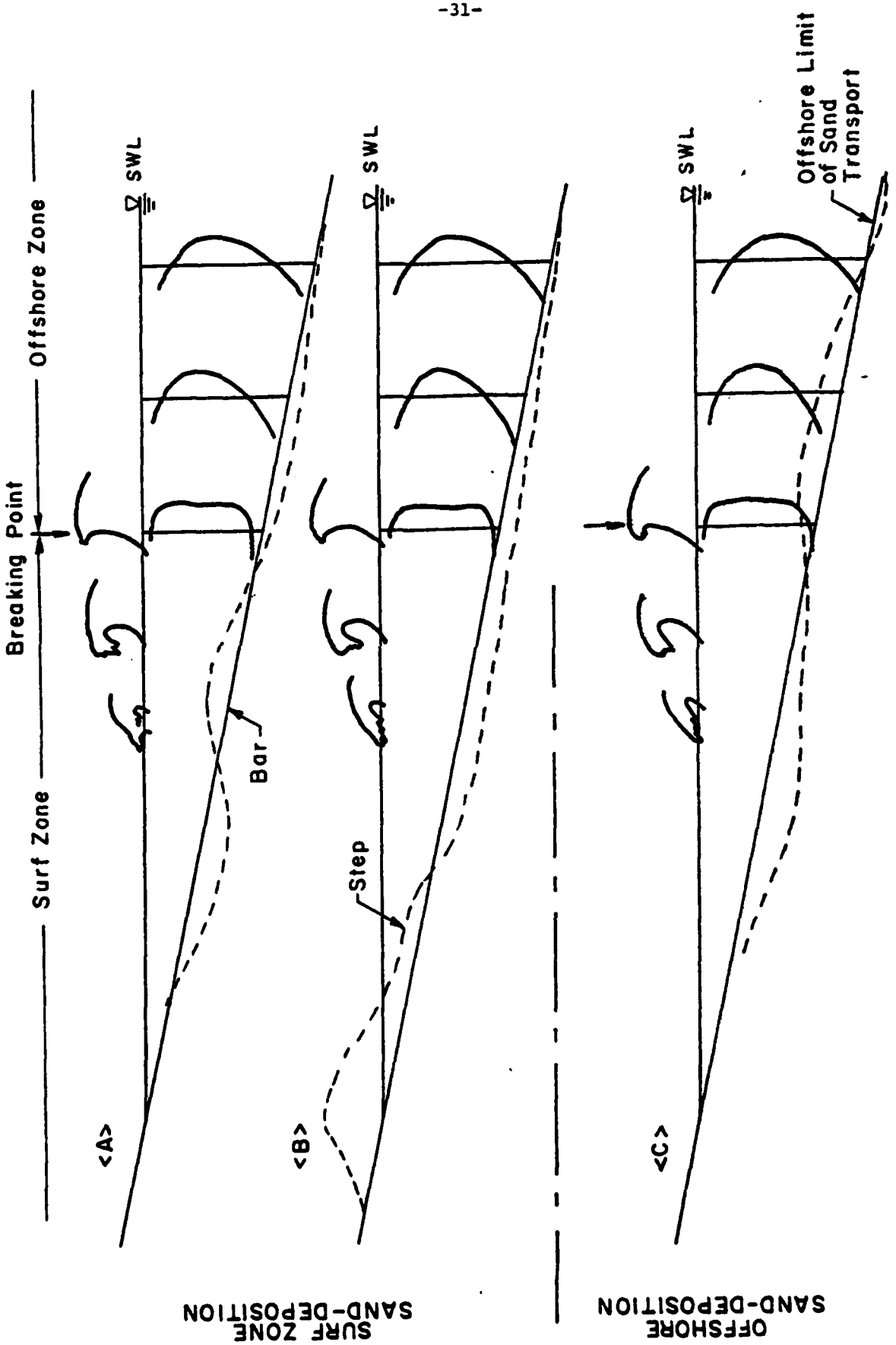

Fig. 11. Types of onshore/offshore sediment transport processes.

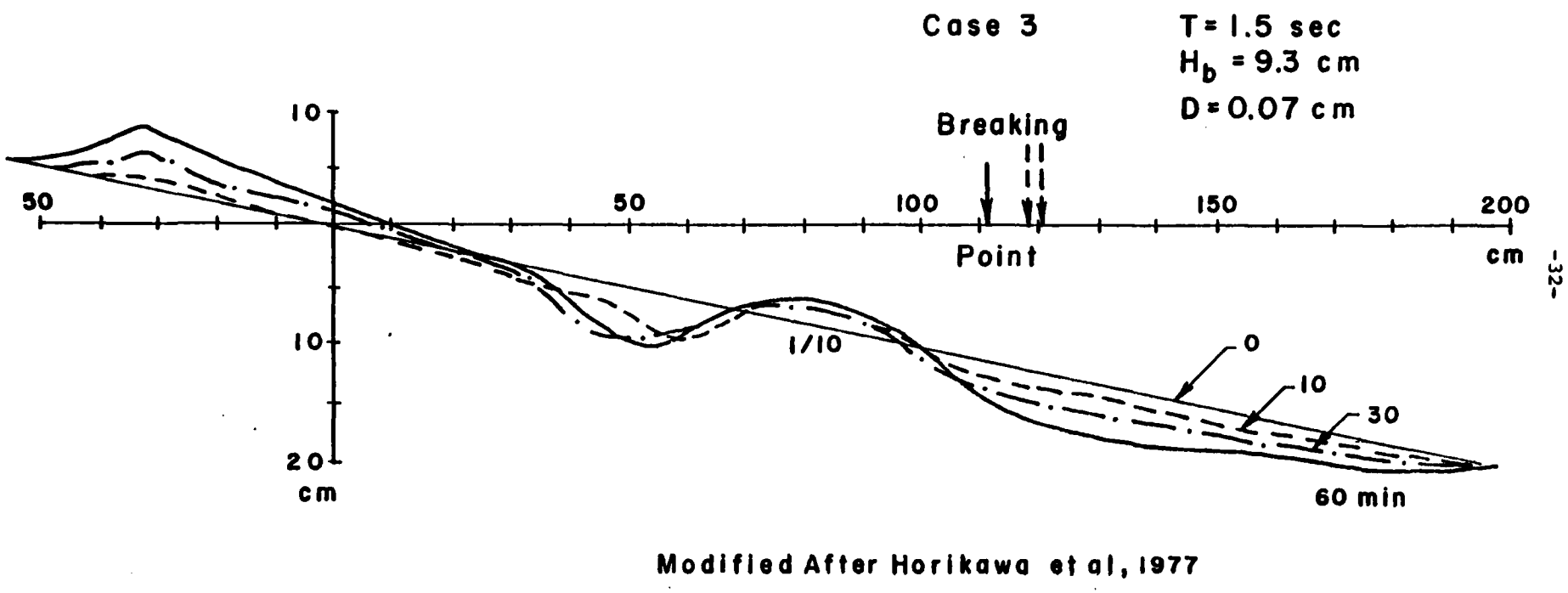

Fig. 12. Onshore sand transport and bar formation inside the surf zone.

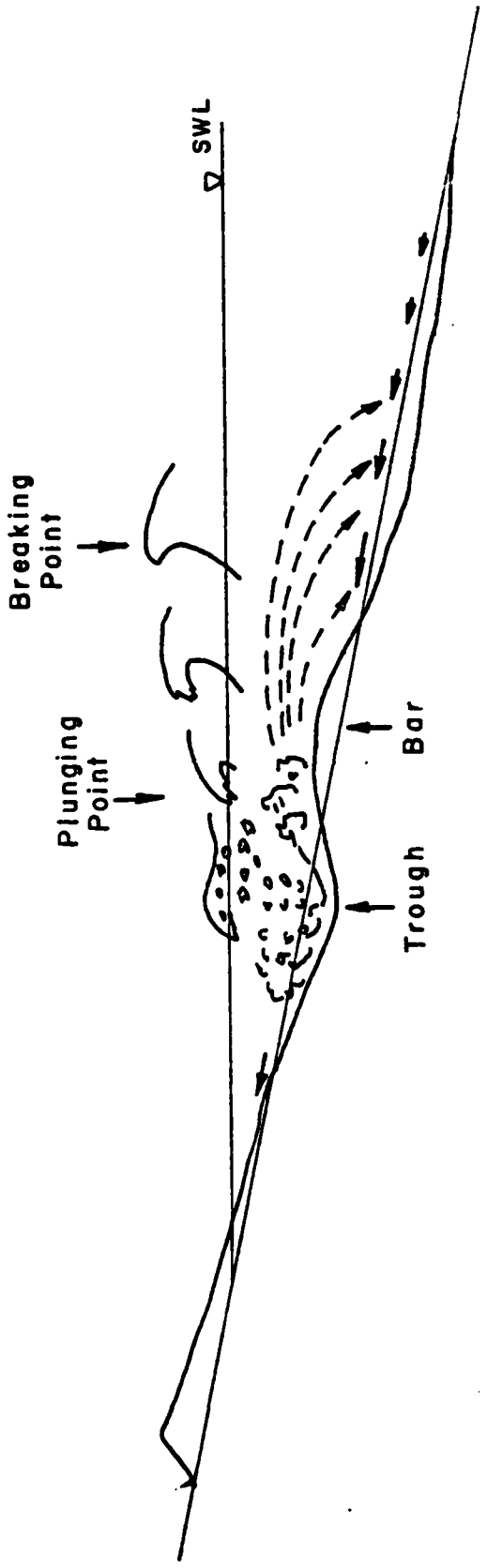

Fig. 13. Possible sand-transport pattern of the case shown in Fig. 15.

If the net offshore sand discharge at the breaking point is larger than the onshore one, then the sand deposition takes place in the offshore region (C in Fig. 11). In this case, there must be an offshore sand-transport limit where the onshore and offshore transport rates become equal, i.e., no further offshore sediment transportation occurs beyond this point.

This offshore transport mechanism, however, gives no clue to the elucidation of continual offshore sand-transportation which is usually observed in a laboratory eroding beach experiment (see Fig. 14). For this type of transportation, the mechanisms of keeping the sand in suspension must exist in the offshore zone. Since the offshore sediment-suspension is initiated by the occurrence of ripple marks, not only mass transport phenomena but also sediment behavior, on and over wave-induced ripple marks, should be scrutinized for the solution of laboratory beach-erosion problems.

V. CONCLUDING REMARKS

Laboratory experiments were conducted to determine the drift velocity at the breaking point on the sloping beach. It was found that, irrespective of breaker types, the drift velocity has onshore direction near the surface and close to the bottom; in the main flow column, the drift velocity is always offshore. The offshore drift velocity shows a more uniform vertical distribution than that in the offshore region. This is probably resulting from the increased momentum transfer due to turbulence at the breaking point. This vertical distribution is very similar whether the breaker is plunging or spilling.

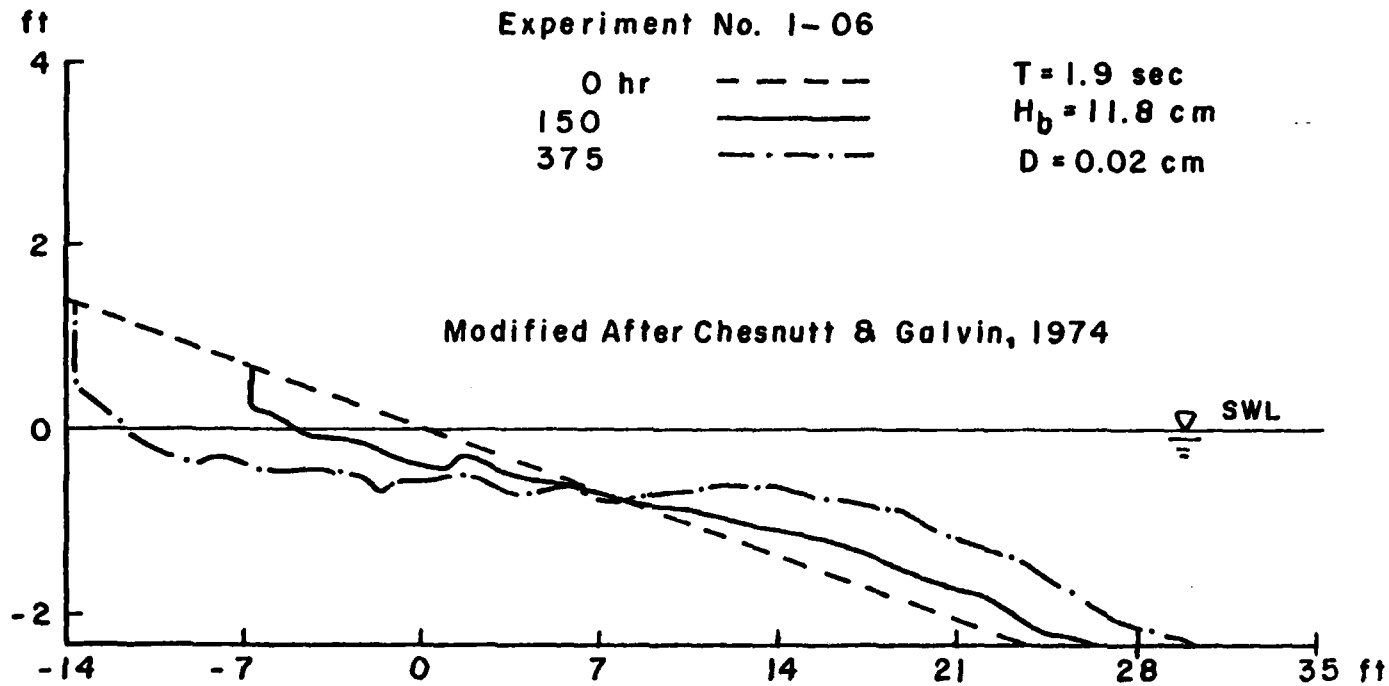

Fig. 14. A typical laboratory eroding beach.

The vertically averaged offshore drift velocity is estimated to be proportional to κ^2 with the constant of proportionality of the order of 0.025-0.030 which is significantly smaller than that predicted by the linear wave theory.

An attempt is made to relate the onshore/offshore sediment transport process with the vertical distribution of mass transport velocity at the breaking point. This relationship is by no means quantitative. Further experiments are needed using movable beds so that the relationship between the sediment movement and the mass transport characteristics can be studied explicitly.

REFERENCES

Bijker, E. W., Kalkwijk, J. P. Th., and Pieters, T. (1974): Mass transport in gravity waves on a sloping bottom. Proc. 14th Conf. Coastal Eng., pp. 447-465.

Chesnutt, C. B. and Galvin, C. J. (1974): Lab profile and reflection changes for H_o/L_o = 0.02. Proc. 14th Conf. Coastal Eng., pp. 958-977.

Dalrymple, R. A. (1976): Wave-induced mass transport in water waves. J. Waterways, Harbors and Coastal Eng. Div., ASCE, WW2, May 1976, pp. 255-264.

Dean, R. G. (1965): Stream function representation of nonlinear ocean waves. J. Geophy. Res., Vol. 79, No. 18, pp. 4561-4572.

Horikawa, K., Sunamura, T. and Shibayama, T. (1977): A laboratory experiment of two-dimensional beach changes. Proc. 24th Jap. Conf. Coastal Eng., pp. 170-174 (in Japanese).

Huang, N. W. (1970): Mass transport induced by wave motion. J. Marine Res., Vol. 28, pp. 35-50.

Liang, S. S. and Wang, H. (1973): Sediment transport in random waves. Tech. Rep. No. 16, College of Marine Studies, Univ. of Delaware, 104 pp.

Longuet-Higgins, M. S. (1953): Mass transport in water waves. Phil. Trans. Roy. Soc. London, Ser. A, Vol. 245, No. 903, pp. 535-581.

Mei, C. C., Liu, P. L. F. and Carter, T. G. (1972): Mass transport in water waves: theory and experiments. Ralph M. Parons Lab. Rep. No. 146, Civil Eng. Dept., MIT, 287 pp.

Russell, R. C. H. and Osorio, J. D. C. (1958): An experimental investigation of drift profiles in a closed channel. Proc. 6th Conf. Coastal Eng., pp. 171-193.

Stokes, G. G. (1847): On the theory of oscillatory waves. Trans. Cambridge Philosophical Society, Vol. 8.


DAT
FILM